



Delta Journal of Basic and Applied Sciences

Available online at Science-Tanta



Research Article

GEOLOGY

Re-Mapping the Neoproterozoic Basement Rocks of Um Gheig area, Central Eastern Desert, Egypt based on Remote Sensing, Petrography and Field Investigation

Mohamed A. Abd El-Wahed^a, El Metwaly Lebda^b, Samir Kamh^a, Mohamed Attia^b

^a Geology Department, Faculty of Science, Tanta University, 31527 Tanta, Egypt

^b Geology Department, Faculty of Science, Kafrelsheikh University, Kafrelsheikh, Egypt

KEY WORDS

ABSTRACT

Um Gheig,
Landsat8(OLI),
CED,
BasementRocks

Landsat 8 (OLI) ETM+ satellite imagery data are evaluated for improving and re-mapping the geologic map of Um Gheig area, Central Eastern Desert of Egypt. Different remote sensing techniques including FCC, band ratio, PCA, supervised classification and spectral characteristic analysis were applied on satellite imagery to facilitate the discrimination of the widely exposed Neoproterozoic basement rocks in the study area. Best color composite 146 FCC, 762 FCC, band ratio 6/2, 4/3, 7/3 and 7/6, 6/5, 4/2 in RGB, as well as PCA 213 and 314 in RGB were selected and used for detailed mapping of the different lithological units. Spectral characteristic analysis was used to discriminate the rock forming minerals through the different rock units in Umm Gheig area (e.g. amphibole b7/b5, serpentine b5/b7, Quartz b7/b6, muscovite b6/b4 and PCA4). The rock units of Um Gheig area are divided four main lithological units according to field and petrographical studies; ophiolitic associations, foliated metavolcanics, post-granitoids and hammamat sediments, as well as small parts of unmappable metavolcanics and metgabbro. Ophiolitic associations are subdivided serpentinites, metagabbro, volcanoclastic metasediments and hornblende schist. Granitoids are subdivided El-Deilihimmi granite and Abu Shaddad granite. Petrographically, serpentinites prevailing by antigirite serpentinites, metagabbro includes quartz and hornblende gabbro, VCM comprised different varieties range from biotite schist, biotite hornblende schist, garnet biotite hornblende schist, intercalations of actionolite schist and highly mylonitic schist, foliated metavolcanics represented by schistose metatuffs and mylonitic schist, metavolcanics represented by meta-andesite and fine metatuff, El-Deilihimmi granite includes granodiorite and monzogranite while Abu shaddad granite comprised alkali feldspar granite and syenogranite, hammamat sediments represented by pebbles of dacite. A new modified geological map is produced for Um Gheig area based on the remote sensing data, field investigation and petrographical description.

1. Introduction

The Arabian-Nubian Shield (ANS) is considered as an example of the East African Orogeny which is consolidated during Neoproterozoic time due to oblique convergence of the intra-oceanic island arcs accretion, continental micro-plates and oceanic plateaus (e.g. Gass, 1982; EL-Gaby et al. 1984, Stren 1993, 1994; Abdelsalam and Stern 1993; Kröner et al., 1994, Abdelsalam and Stern, 1996, Fritz et al. 1996, Bregar et al. 2002, Abdeen and Greiling 2005, Abd El-Naby and Frisch 2006, Abd El-Wahed 2008, Ali et al. 2010, Shalaby 2010, Abd El-Rahman et al. 2012, Fritz et al. 2013). It is from the NE part of Africa (Kröner 1984, Abdelsalam and Stren 1993). Several authors agree that the Egyptian Eastern desert includes Neoproterozoic rocks that form part of the Arabian–Nubian shield (EL-Gaby et al. 1984, Abdelsalam and Stern 1993, Fritz et al. 1996, Bregar et al. 2002, Fritz et al. 2002, Abdeen and Greiling 2005, Abd El-Naby and Frisch 2006, Abd El-Naby et al. 2008, Abd El-Wahed 2008, Ali et al. 2010, Shalaby 2010, Abd El-Rahman et al. 2012 and Fritz et al. 2013).

The Eastern Desert of Egypt forms the northwestern part of the Arabian–Nubian Shield (ANS) and consider the northern extension of the East African Orogen (Abd El-Rahman et al. 2012). Stern and Hedge (1985), divided the Neoproterozoic rocks of the Eastern Desert of Egypt into three tectonic domains: the

Northern Eastern Desert (NED), the Central Eastern Desert (CED), and the Southern Eastern Desert (SED). The major exposure of Neoproterozoic rocks widely located in the Central Eastern desert (CED) due to the flank uplift triggered by the Red Sea rift (Garfunkel, 1988; Omar et al., 1989). El-Gaby et al. 1988; Abdeen and Greiling 2005; Abd El-Wahed and Kamh 2010 divided the rock units of CED into two main tectonostratigraphic units lower unit that known by the infrastructure (El-Gaby et al., 1990) and consist of medium to high-grade gneisses and migmatites which exposed as dome structures (Habib et al., 1985 and El-Gaby et al., 1990), like, Sibai, Meatiq, and Hafafit domes and upper unit that known by suprastructure (El-Gaby et al., 1990) or Pan-African Nappe Complex (Fritz et al., 1996, 2002; Bregar et al., 1996, 2002; Fowler and El-Kalioubi, 2004) composed of Low-grade island arc-related metavolcanic, metasedimentry and ophiolite complexes of Neoproterozoic age as well as they form the largest part of the Neoproterozoic rocks exposed in the Eastern Desert (Gass, 1982; Stern, 1994; Kröner et al., 1994, Neumayr et al., 1998).

Urn Gheig area is delimited by the latitudes (25° 39' N and 25° 45' N), longitudes (34° 20' E and 34° 29' E) and located at the central part of the Eastern Desert of Egypt

about 7 km inland from the Red Sea coast of Egypt and 52 km south of Quseir city (Fig. 1).

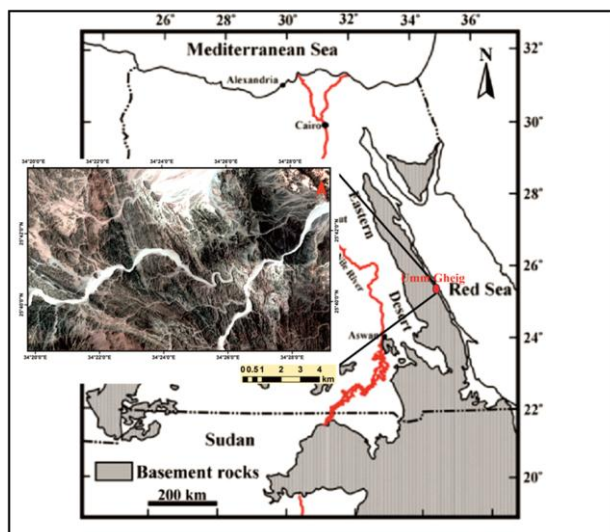


Fig. 1: location map of Um Gheig area. Inset: Landsat 8 (OLI) image RGB-321.

Many authors e.g. [El-Anwar \(1983\)](#), [Stern and Hedge, \(1985\)](#); [El-Gaby et al., \(1988\)](#) and [\(1990\)](#); [Hassan and Hashad \(1990\)](#), studied the geological setting of the study area and considered that area, as a part of the Arabian Nubian Shield, was subjected to the Pan African Orogeny. The geological and geochemical studies by [Asran \(1991\)](#) of Wadi Um Gheig area revealed that the area mapped as ophiolitic rocks, which comprise serpentinites and metagabbros thrust over island arc metavolcanics.

[El-Anwar \(1983\)](#) presented a detailed geologic map of the study area and concluded that the area is covered by amphibolites, greenschists, serpentinites, metagabbros, younger granites and Hammamat sediments.

[Ibrahim and Cosgrove \(2001\)](#) studied Wadi Um Gheig/El-Shush area and divided the rocks into three units: i) low-grade metamorphosed rocks, which consist of metavolcanic rocks interleaved with slices of ophiolitic melange; ii) high-grade metamorphic rocks, which consist of syn-tectonic granitoids; iii) Post-tectonic granites, which intrude into both the low- and high-grade rocks. [El Bahariya et al. \(2001\)](#), studied the previous three rock units of Umm Luseifa metavolcanics. They concluded that each unit comprise number of rock units as the following: The metamorphosed mafic rocks which form the Eastern, South-eastern and north-western part of the mapped metavolcanics included: a) Tuffaceous metabasalt; b) Mafic crystal tuff; c) Hornblende and hornfel and amphibolites. [Abdeen \(2003\)](#), mapped the rock units of study area as Pan-African nappe complex includes ophiolitic mélangé and related metavolcanic and metasedimentary rocks.

The origin of ophiolitic rocks in Wadi Wizr was investigated by [Abdel-Karim and Ahmed \(2010\)](#). They considered that the ophiolitic sequence comprised serpentinites, talc-carbonate rocks, metagabbros, metapyroxenites and metabasalts. The Pan-African rock associations of the Um Gheig-Kadabora area has been divided by [Abdeen et al. \(2014\)](#) into two lithological units: lower unit that consist mainly of amphibolite-migmatite and granitoid gneisses, and an upper unit that comprised ophiolitic rocks, metavolcanics and

their related volcanoclastics, and molasse-type Hammamat sediments. [Abu El-Leil et al. \(2017\)](#) studied the structural elements and geological setting of Um Gheig area. They divided the rock units of the area into a) upper crust (oldest) comprises the low to medium grade metamorphic rocks of ophiolite and island arc rock units represented by the serpentinites, metavolcanosedimentary rocks, metavolcanics and metagabbros; b) lower crust of high grade metamorphic rocks including migmatite, gneissic tonalite, tonalite-granodiorite and sheared granite; c) late to post orogenic magmatism (youngest) represented by biotite granite, alkali feldspar granite and fresh gabbro..

The main aim of this work is to produce new detailed and modified geological map of Um Gheig area using mainly, the remote sensing data, in addition to field and petrographical investigations to verify the obtained results from Landsat images.

Lithological mapping based remote sensing

Remote sensing considered an important mapping tool in the past several decades and it finds applications in geological and structural mapping, particularly as a complementary source of information in conjunction with field work. Remote sensing together with Geographic Information System (GIS) technologies provides better opportunities to prepare geological maps with higher accuracy. A suitable analysis of satellite optical images like Landsat 8 (OLI) data substantially helps in lithological investigation

of poorly understood areas and to improve the published maps which mapped by the traditional techniques. Mainly, geologic mapping is planned to refine the geological boundaries, structural elements and distinguished between the different rock units of the studied area. The production of the geological map has been carried out using analyzed satellite image, in addition to field work and microscopic and geochemical analyses. Various band ratio, false color composite images (FCC) and principle component analyses (PCA) as well as supervised classification are used for the detailed lithological mapping of the study area.

Colour composite defined as an image produced by displaying multiple spectral bands as colours different from the spectral range in which they were taken. This method is commonly used for displaying multi-band (multi-channel) imagery. This is usually achieved by assigning three of the image bands to the fundamental colours red (R), green (G) and blue (B), the combination of which results in a RGB (false) colour composite image. [Chica-Olmo et al. \(2002\)](#), stated that RGB colour composition is a basic procedure for geological photointerpretation applications in which groups of bands are selected depending on the features to be enhanced.

Band ratio considers another useful approach for separating different lithological units is the application of band ratios to the Landsat bands (band ratioing). [Lillesand and Kiefer, 1979](#) and [Sonka et al., 1993](#) stated ratio

images are enhancements resulting from the division of DN values in one spectral band by corresponding values in another band.

Principal component analysis (PCA) is a multivariate statistical technique used to reduce the data redundancy by transforming the original data onto new principal component axes producing an uncorrelated image, which has much higher contrast than the original bands (Crosta and Moore 1989, Loughlin 1991). Statistical analyses displayed that the first three components contain more than 97% of the total variance. A three- band PC coloured composite was shown with PC1= red, PC2= green and PC3= blue.

Kamel et al., (2016) defined **image classification** as a process by which pixels having similar spectral characteristics are consequently assumed to belong to the same class that can be identified and assigned a unique color. There are two main spectrally oriented classification procedures for land cover mapping: unsupervised and supervised classifications.

Supervised classification defined by Lillesand and Kiefer (2000), as a process where the classifier or image analyst supervises the pixel categorization processes by specifying to the computer algorithm, numerical descriptors of the various land cover types present in a scene.

Spectral characteristic analysis

It is accepted that each material in nature has a characteristic spectral reflectance curves that distinguish it from others. This characteristic represents the basis for identifying, and distinguishing the different minerals and rocks from satellite images. The final spectra of rocks are consisting of interference, and stacking of the spectra of their constituent minerals, and change from rock to another based on mineral composition. The examined average Digital Number (DN) values of the response of the widely exposed lithologies of both Landsat 8 bands is successfully used in predicting the effective band ratios to emphasize between the different lithologies in Umm Gheig area based on mineral index through each rock unit.

Data Used and Methodology

The satellite data used in the present study originates from Landsat 8 (OLI) ETM+, which is frequently used for geological mapping with satisfy scale. Landsat 8 (OLI) scene with Path 174/Row 042 and cloud cover 0.01 was used in the present study. The data were georeferenced to Universal Transverse Mercator (UTM), World Geodetic system 1984 (WGS 84) zone 36. The used RS Landsat 8 (OLI) satellite images were obtained free from Image courtesy of the U.S. Geological Survey (USGS) earth explorer website (<http://earthexplorer.usgs.gov>) having an acquisition date of June 26, 2016.

The pre-processing and processing of the Landsat 8 (OLI) scene data covering the area was performed by using the ENVI 5.3 and ArcGIS 10.5 software. The pre-processing techniques of radiometric and atmospheric corrections were performed.

The output results of the remote sensing mapping and mineral detections were integrated and validated by the field investigation, and petrographical studies.

Besides the field and petrographical investigation as well as different combinations of Landsat bands, various band ratios used as mineral index for mineralogical discrimination of the lithological (e.g. 4/2, 7/5, 5/7, 7/6, 6/4 and 6/5 after [Hassan et al. 2017](#)).

The results and discussion

Field and petrographical investigations

The study area dissected by several wadis (e.g. W. Um Gheig, W. Umm Luseifa, W. Wizar, W. Kab Ahmed and W. Umm shaddad) which drain into the Red Sea to the east. The relief of the study area characterized by the variation which range from 46 m to 1490 m above sea level. The granitic units represent the highest relief in the area that reaching to 1490 meters above sea level of Gabal El-Sibai and 776 meters above sea level of Gabal Umm Shaddad.

According to the Field studies and petrographic description, the study area can divided into four main rock units, they are from the oldest to the youngest: ophiolitic associations, foliated metavolcanics, granitoids and Hammamat

sediments as well as some un-mappable units of metagabbros and metavolcanics.

Ophiolitic associations considered the oldest rock unit and form the largest part of the study area. Based on the field and petrographic investigation, the ophiolitic association subdivided into serpentinites, metagabbros, volcanoclastic metasediments and hornblende schist.

Serpentinites occurred as blocks at the northeastern part of the study area as well as small blocks at the south side of the central part of the study area (Figs. 2a and 7). Microscopically, serpentinites comprised Antigorite serpentinite with pyroxene relics, antigorite serpentinite and talc carbonate serpentinites. It is characterized by the prevailing of antigorite as well as some of carbonates, iron oxides and chromites (Fig. 3 a and b).

Metagabbros occurred as mappable blocks at the northeastern corner of the study area (Fig. 2b and 7) and petrographically divided into hornblende metagabbro and quartz metagabbro. Metagabbros consists mainly of hornblende, actinolite, plagioclase; secondary minerals are sericite and epidote; minor of quartz while the accessory minerals represented by calcite and opaque minerals (Fig. 3c). Quartz occurs as a major content in quartz metagabbro.

Volcanoclastic metasediments occurred as along belts that occupy the central part and southwestern corner of the study area (Fig. 2c and 7). Microscopic investigation shows that the volcanoclastic metasediments includes

biotite schist, biotite hornblende schist, garnet biotite hornblende schist and intercalations of actinolite schist (Fig. 3d, e and f). Hornblende schist occurred as intensive foliated unit with dark green color at the northwestern part and southwestern corner of the study area (Fig. 2d) as well as it composed mainly of hornblende, actinolite and uartz crystals, besides some spots of calcite and iron oxides (Fig. 3g). These units characterized by the quartz, hornblende, actinolite, biotite, muscovite and garnet as a main minerals content and by chlorite and iron oxides as a secondary minerals content.

Foliated metavolcanics exposed as long foliated belts located at eastern side and north central part of the study area, the intensity of foliation decrease toward the entrance of Wadi Um Gheig (Fig. 2e). Microscopically, foliated metavolcanics comprised schistose metatuffs and mylonitic schist (Fig. 3h). They composed variable clasts of quartz, plagioclase, k-feldspars (orthoclase) as main minerals and sericite chlorite, carbonates (calcite) and opaque minerals as a secondary minerals. While unmaple metavolcanics exposed in some places through some parts of the study area as low hills (Fig. 2f) and subdivided according to microscopic investigation into meta-andesite and fine metatuff (Fig. 3i). They characterized by quartz, plagioclase, orthoclase and chlorite as secondary minerals.

Granitoids exposed as high relief belts at the northwestern corner intruded through the oldest units like hornblende schist and volcanoclastic metasediments. These granitoids represented by El-Delihimmi granite that includes cataclastic monzogranite and granodiorite as well as syenogranite and alkalifeldspar granite of Gebel Abu Shaddad (Fig. 2g and h). Monzogranite characterized by the prevailing of plagioclase as well as quartz, K-feldspars and mica (Fig. 3j), while syenogranite and alkalifeldspar granite marked by the prevailing of K-feldspars and perthite as well as quartz, plagioclase and mica (Fig 3k).

Hammamat sediments are occupying the southeastern corner as low relief hills with large pebbles of chert (Fig. 2i) and represented by conglomerate, felsites and basalt. The pebbles and boulders of conglomerates includes dacite which composed mainly of phenocryst (plagioclase and quartz) and groundmass or matrix of fine plagioclase, quartz and some lithic fragments (Fig. 3l).

Remote sensing interpretation

FCC 126 in RGB considered one of the best false composite, which separated the serpentinite blocks with dark olive green color and metabbabros with black blue color at the northeastern part of the mapped area (Fig. 4a). Foliated metavolcanics separated obviously in FCC 762 in RGB with reddish brown color at the entrance of Wadi Umm Gheig and with whitish pale violet in Wadi Wizr as well as Hammamat sediments that marked by dirty

dark green at the southeastern corner of the study area (Fig. 4b).

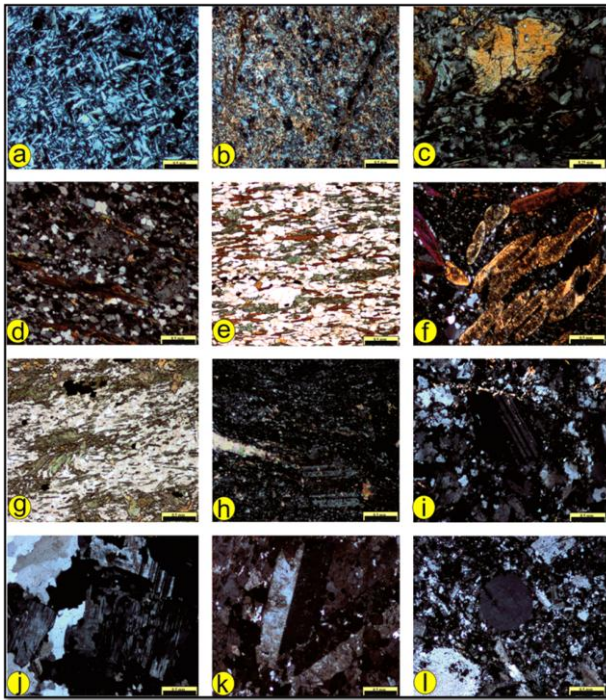


Fig. 3: photomicrographs of a) Antigorite Serpentinite shows antigorite mineral with flame habit or flake shape and exhibit mesh texture and disseminated grains of iron oxides (CN); b) Talc Carbonate Serpentinites includes antigorite of tiny flake shape and several scattered patches of carbonates which replaced most of the antigorite beside, disseminated iron oxides (CN); c) Hornblende metagabbro contains hornblende crystal show two set of cleavage and has inclusions of plagioclase that reflect ophitic and subophitic texture as well as chlorite crystals that appear as flakes (CN); d) Biotite Schist comprised biotite flakes and associated minor muscovite oriented in parallel alignment exhibiting the schistose texture and anhedral crystals of quartz (CN); e) Biotite Hornblende Schist shows alternative bands of quartz, biotite and hornblende oriented in parallel alignment exhibiting the schistose texture (PPL); f) Actinolite Schist exhibits aggregate of euhedral prismatic crystals of actinolite oriented in the same direction and have inclusions of quartz (CN); g) Hornblende Schist contains hornblende and actinolite crystals which some of them parallel to foliation and the others oriented randomly away the foliation direction (PPL); h) Schistose Metatuffs shows large plagioclase crystal occur as porphyroblast which the matrix wrapped around it (CN); i) Meta-andesite displays corroded subhedral crystal of plagioclase exhibits albite twinning and embedded in a groundmass of quartz, plagioclase and fine saussuritized plagioclase crystals identifying the porphyritic texture (CN); j) Monzogranite includes group

of fresh subhedral plagioclase crystal with corroded borders exhibiting albite twinning (CN); k) Alkalifeldspar Granite shows subhedral orthoclase crystals with simple twinning and inclusions like the flame identifying the perthite texture (CN); l) Dacite contains well rounded quartz crystal enclosed in a groundmass of fine plagioclase and quartz crystals (CN).

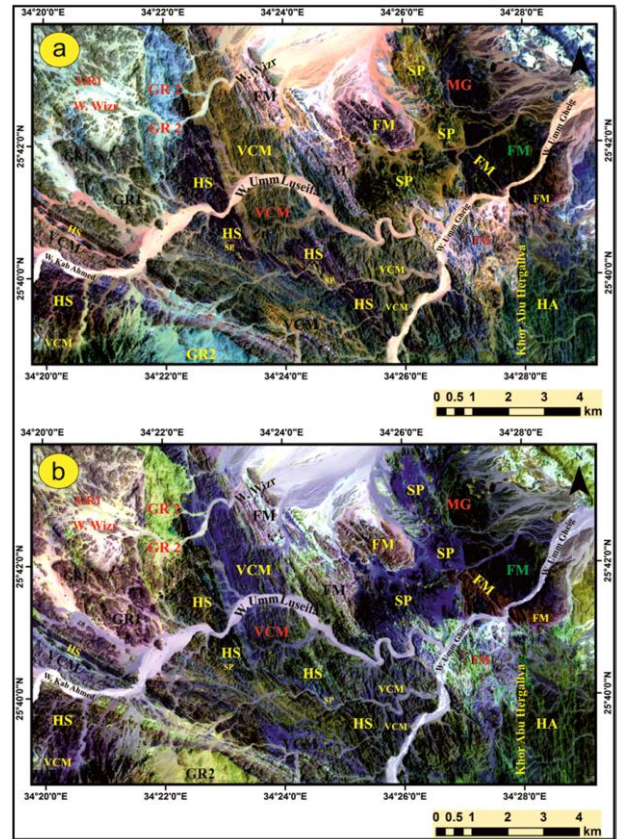


Fig. 4: False color composites (FCC), a) 126 in RGB; b) 672 in RGB of landsat 8 (OLI). The discriminated rock units include serpentinites (Srp), metagabbro (MG), highly foliated metavolcanics (HFM), hammamat sediments (HS), volcanoclastic metasediments (VCM), hornblende schist (HS), monzogranite (MonG) and granodiorite (GD).

This band ratio separated and marked each rock units with special color (e.g. HFM: yellow to greenish yellow, Srp: deep black blue, MG: green, VCM: pinkish violet, HS: yellowish green, HS: pinkish blue, MonG: canyon and GD: pink).

The principal component analysis (PCA) 213, in RGB discriminated the ophiolitic associations with pink color except HS appears with pinkish deep blue color, while HFM appears with blue to pale blue color and MonG with green color as well as HS marked with pinkish orange color (Fig.6a). Highly foliated

metavolcanics and different types of granites as well as metagabbros discriminated obviously in PCA 314, in RGB (Fig.6b), which HFM marked by red color at the entrance of Wadi Um Gheig while through Wadi Um Gheig and Wadi Wizr appears with canyon red to canyon color, monzogranite marked by green color while granodiorite marked by orange color and metagabbros deep blue color.

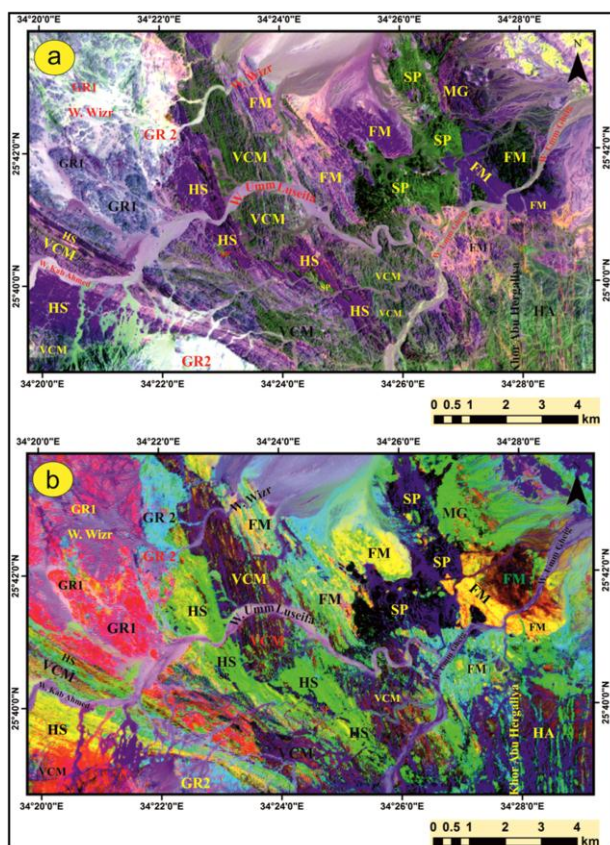


Fig. 5: Band ratios combinations: (a) 6/2, 4/3, 7/3 and (b) 7/6, 6/5, 4/2, in RGB of landsat 8 (OLI), for abbreviations see (Fig. 4).

The produced supervised classification map in Figure (7) offered an obvious and easily discrimination of the different rock units and trace the geological boundaries sharply. The new classified map is used as an improved geologic map of the study area.

The prepared geological map shows clear improvements and variations to the earlier version of [El-Anwar \(1983\)](#) Fig (8) and [Abu El-Leil et al. \(2017\)](#). The old geologic maps were improved and refined distinctly, giving more precise borders, a higher resolution and a better exclusion of ophiolite assemblage and granitic rocks. Many borders between the lithological units were set up new, while other predicted borders were confirmed. Moreover, the discrimination between several rock types was enhanced, e.g. the contact between serpentinites and metagabbros become visible (Fig. 8 (1)). Obviously, some regions are reclassified as different unit than before, the belt of amphibolite are reclassified to HB schist and volcanoclastic metasediments.

Where the HB schist was enhanced clearly by different remote sensing techniques by a sharp contact with the volcanoclastic metasediments (Fig. 8 (2), (3)). In the southwestern part of the study area [Abu El-Leil et al. \(2017\)](#) mapped the area around Wadi Kab Ahmed as metavolcanosedimentary rocks but the present study added the hornblende schist as an elongated slab in the volcanoclastic metasediments (Fig. 8 (2)). The greenschist of [El-Anwar \(1983\)](#) is confirmed and re-mapped by remote sensing and petrography as a foliated metavolcanics (Fig. 8 (4)). The granitic rock body in the northwest of the study area (Gabal El Deilhimmi area) is differentiated into two phases of granites as a granodiorite and monzogranite (Fig. 8 (5)). This is confirmed by

the petrography and mineral indices of remote sensing .

It seems be that the new geologic map is clear and trustworthy, especially the new lithologic units added and sharp contact enhanced by the integrated interpretation of the remote sensing data and petrographical study as well as the serious field work investigations.

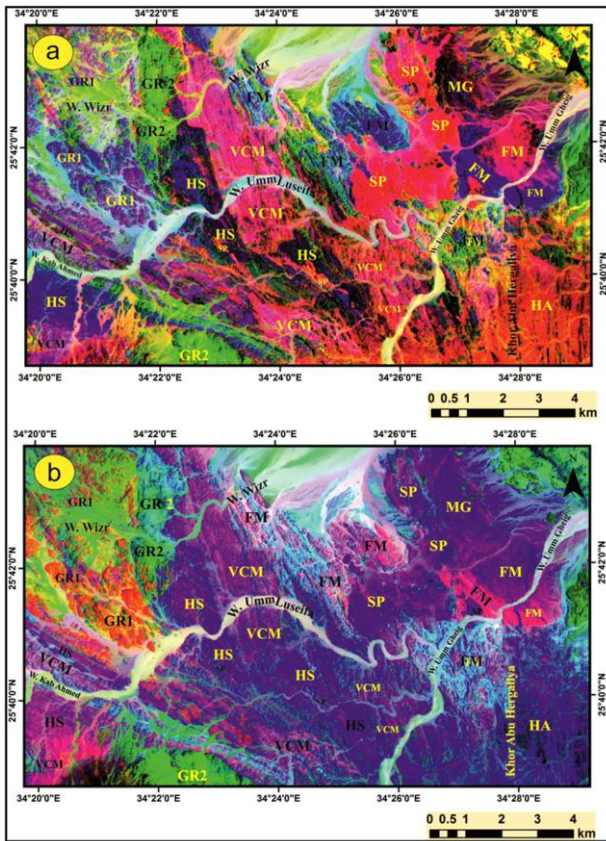


Fig. 6: PCA, a) 213, in RGB, b) 314, in RGB of landsat 8 (OLI), for abbreviations see (Fig. 4).

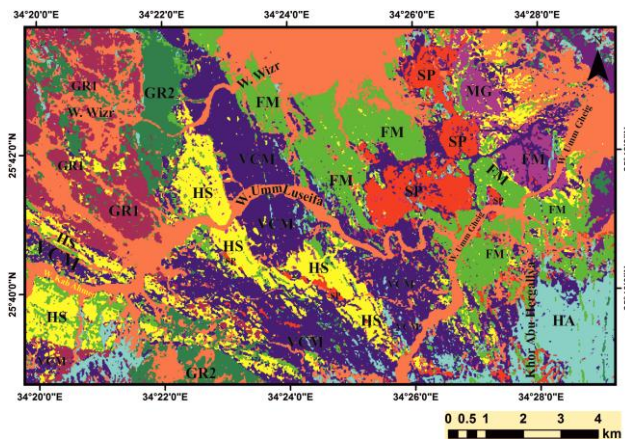


Fig. 7: Supervised classification used to improve the geologic map of W. Umm Gheig area to

produce new detailed geological map, for abbreviations see (Fig. 4).

Mineral detection

The grey scale of Landsat-8 ratio image b7/b5 was used as an effective tool to emphasize rocks rich by amphibole, which appears with bright tone (Fig. 9a). The grey scale Landsat-8 ratio image b5/b7 image was success to discriminate of serpentines minerals that appears with bright tone (Fig. 9b). Where band ratio of b4/b2 used to distinguishes the rocks rich by iron oxides like hematite, magnetite, limonite, and appears with dark tone (Fig. 9c).

Muscovite mineral distinguished by b6/b4 ratio image in gray scale as a marker to mylonitic and granites that exposed with bright tone (Fig. 9d). The gray scale ratio b7/b6 and PCA4 used to emphasize the rock units rich by silica (quartz mineral) which appears with bright tone (Fig. 9e) and dark tone (Fig. 9f). PCA4 considered good indicator for granitic rocks.

Conclusions

Using the integrated approach of remote sensing, petrography and fieldwork, it was possible to improve and re remap the geological map of Um Gheig area. The former publications, many of them showed up fair results with small scale. The present approach of using remote sensing, petrography and fieldwork reached promising results, giving a good contrast and discriminability of occurring rock types. In remote sensing, the attempt of choosing the best suitable PC bands by analyzing their eigenvector loadings and

contrast gained good results as well. The chosen principal components PCs gave a better lithological discrimination. It was possible to enhance the remote sensing classification quality by the petrography and fieldwork. The accuracy was notably increased compared to the usage of only one type of data. The main part of the present study area reaches excellent classification results and the borders between lithological units are clear especially in the foliated rock units and granitic bodies.

Based on field investigation and petrographical descriptions, the rock units of Um Gheig area divided into four main lithological units, they are ophiolitic associations, foliated metavolcanics, post-granitoids and Hammamat sediments, as well as small parts of unmapple metavolcanics and metagabbro. Ophiolitic associations subdivided into serpentinites, metagabbro, volcanoclastic metasediments and hornblende schist. Granitoids subdivided into El-Deilihimmi granite and Abu Shaddad granite.

In present study, the remote sensing offered the best color composite FCC 146, FCC 762, band ratios of 6/2, 4/3, 7/3 and 7/6, 6/5, 4/2 in RGB and PCA 213 and 314 in RGB, were successfully discriminate the Neoproterozoic basement rocks with sharp contacts and tones. In addition, some mineral indices are used to enhance the felsic and mafic mineral content of some rocks. Amphibole index is good indicator to hornblende schist.

Serpentine index is a good marker to serpentinites and altered ultramafic rocks. Muscovite index discriminate mylonitic schist and granites as well as quartz index is distinguishing the rocks rich by silica (Felsic, meta-felsic and metasediments) through the study area. Finally, the present study offered a new and improved geologic amp of Wadi Um Gheig area with considerable modifications and large scale.

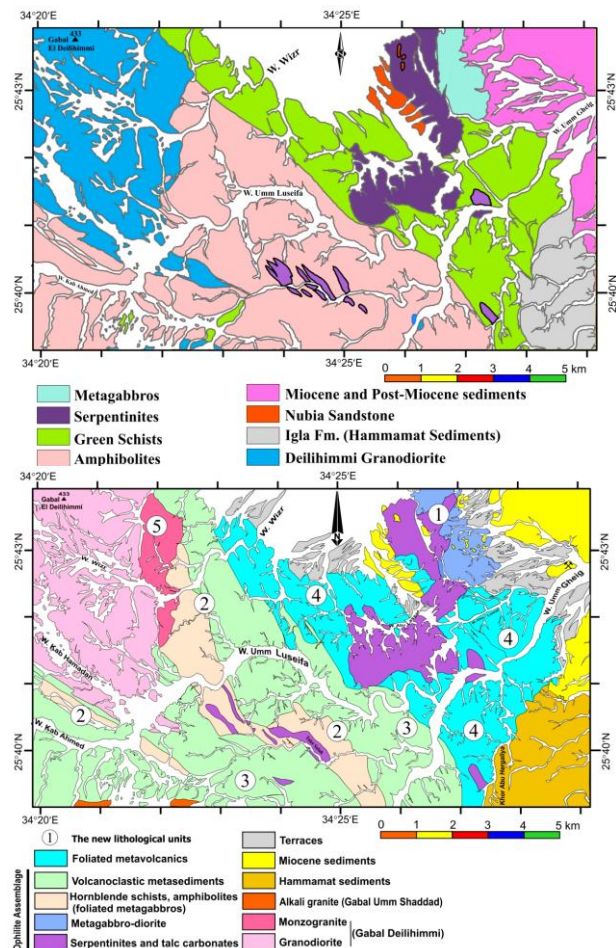


Fig. 8: Comparison between the former geological map of Um Gheig area (after El-Anwar, 1983, (above) and the improved version prepared in the present study (below).

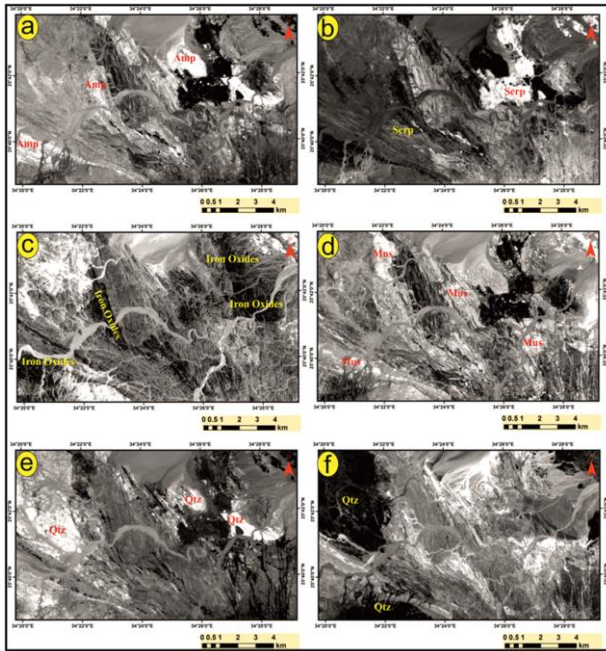


Fig. 9: a) band ratio 7/5 in gray scale for amphibole (Amp); b) band ratio 5/7 in gray scale for serpentines (Serp Index); c) band ratio 4/2 in gray scale for iron oxides (Iron oxides); d) band ratio 6/4 in gray scale for muscovite (Mus); e) band ratio 7/6 in gray scale for quartz, after Hassan et al. (2017) (Qtz); f) PCA4 in gray scale for granites (Qtz).

References

Abd El-Karim, A. M. and Ahmed, Z., (2010). Possible origin of the ophiolites of eastern desert, Egypt, from geochemical Perspectives. *The Arabian Journal for Science and Engineering*, Volume 35, Number 1A.

Abd El-Naby, H. and Frisch, W., (2006). Geochemical constraints from the Hafafit Metamorphic Complex (HMC): evidence of Neoproterozoic back arc basin development in the central Eastern Desert of Egypt. *Journal of African Earth Sciences* 45, 173–186.

Abd EL-Naby, H., Frisch, W. and Siebel, W., (2008). Tectono-metamorphic evolution of the Wadi Hafafit Culmination (central Eastern Desert, Egypt). Implication for Neoproterozoic core complex exhumation in NE Africa. *Geologica Acta* 6/4, 293–312.

Abd El-Rahman, Y., Polat, A., Dilekd, Y., Kuskye, T., El-Sharkawia, M. and Saida, A., (2012). Cryogenian ophiolite tectonics and metallogeny of the Central Eastern Desert of Egypt. *Int. Geol. Rev.* 54 (16), pp.1870–1884.

Abd El Wahed, M., (2008). Thrusting and transpressional shearing in the Pan-African

nappe southwest El-Sibai core complex, Central Eastern Desert, Egypt. *Journal of African Earth Sciences* 50, 16–36.

Abd El-Wahed, M. A. and Kamh, S. Z., (2010). Pan-African dextral transpressive duplex and flower structure in the Central Eastern Desert of Egypt. *Gondwana Res.* 18, pp. 315–336.

Abdeen, M. M., (2003). Tectonic history of the Pan-African orogeny in Umm Gheig area, Central Eastern Desert. *Egypt J Geol* 47(1):239–254.

Abdeen M. M. and Greiling R.O., (2005). A quantitative structural study of late Pan-African compressional deformation in the Central Eastern Desert (Egypt) during Gondwana assembly. *Gondwana Research* 8(4):457–471.

Abdeen., M. M., Greiling, R. O., Sadek, M. F. and Hamad, S. S., (2014). Magnetic fabrics and Pan-African structural evolution in the Najd Fault corridor in the Eastern Desert of Egypt. *Journal of African Earth Sciences* 99, 93–108.

Abdelsalam M. G. and Stern R. J., (1993). Tectonic evolution of the Nakasib suture, Red Sea Hills, Sudan: evidence for a late Precambrian Wilson Cycle. *Journal of the Geological Society, London*, Vol. 1150, 1993, pp. 393-404.

Abdelsalam, M. G. and Stern, R. J., (1996). Sutures and shear zones in the Arabian–Nubian Shield. *Journal of African Earth Sciences* 23, 289–310.

Abu El-Leil, I., Bekiet, M. H., Soliman, N. M. and El-Hebiry, M. S., (2017). Compressional - Extensional Deformation on the Neoproterozoic Rocks, Eastern Desert, Egypt: A Geological And Structural Complementary Study Of Um Gheig Area. *Al Azhar Bulletin of Science* Vol. 9th., p. 1-24.

Ali, K. A., Azer, M. K., Gahlan, H. A., Wilde, S. A., Samuel, M. D. and Stern, R. J., (2010a). Age constraints on the formation and emplacement of Neoproterozoic ophiolites along the Allaqi–Heiani Suture, South Eastern Desert of Egypt. *Gondwana Research* 18, 583–595.

Ali, K. A., Stern, R. J., Manton, W.I., Kimura, J. I., Whitehouse, M. J., Mukherjee, S. K., Johnson, P. R. and Griffin, W. R., (2010b). Geochemical, U-Pb zircon, and Nd isotope investigations of the Neoproterozoic

Ghawjah Metavolcanic rocks, Northwestern Saudi Arabia. *Lithos* 120, 379–392.

Asran, M. H. A., (1991). Geology of Wadi Um Gheig area, Eastern Desert of Egypt. Ph. D. dissertation 276~. Assiut University, Assiut, Egypt.

Bregar, M., Fritz, H., and Unzog, W., (1996). Structural evolution of low-angle normal faults SE of the Gebel El-Sibai Crystalline Dome; Eastern Desert, Egypt: evidence from paleopiezometry and vorticity analysis. *Zbl. Geol. Palaont. Teil I, H. 3/4*, 243–256.

Bregar, M., Bauernhofer, A., Pelz, K., Klotzli, U., Fritz, H. and Neumayr, P., (2002). A late neoproterozoic magmatic core complex in the Eastern Desert of Egypt; emplacement of granitoids in a wrench-tectonic setting. *Precambrian Research* 118, 59–82.

Chica-olmo, M., Abarca, F., and Rigol, J. P., (2002). Development of a Decision Support System based on remote sensing and GIS techniques for gold-rich area identification in SE Spain, *International Journal of Remote Sensing*, 23:22, pp. 4801-4814.

Crosta, A. P., Moore, J. M., 1989. Enhancement of Landsat Thematic Mapper imagery for residual soil mapping in SW Minas Gerais State, Brazil: a prospecting case history in Greenstone belt terrain. In: *Proceedings of the 7th ERIM Thematic Conference. Remote Sensing and Exploration Geology*, pp. 1173e1187.

El-Anwar M. A., (1983). Geology of the area around Wadi Um Gheig, Eastern Desert, Egypt. M. SC. Thesis, Tanta University.

El-Bahariya G. A., Abd El-Wahed M. A. and Abu Anbar M. M., (2001). Petrology, mineral chemistry and deformational-metamorphic history of Um Luseifa composite metavolcanics, Central Eastern Desert, Egypt. *The Second International Conference on the Geology of Africa*, Assiut University, Assiut, 28–30 October 2001, Egypt 1A, 177–204.

El Gaby, S., El Nady, O. and Khudeir, A. A., (1984). Tectonic evolution of the basement complex in the central Eastern Desert. *Geologische Rundschau* 73, 1019–1036.

El Gaby, S., List, F. K. and Tehrani, R., (1990). The basement complex of the Eastern Desert and Sinai. In: Said, R. (Ed.), *The*

Geology of Egypt. Balkema, Rotterdam, pp. 175–184.

El-Gaby, S., CISI, K. and Tehrani, R., (1988). Geology, evolution and metallogenesis of the Pan-African belt in Egypt. In: El-Gaby, S., Greiling, R.O. (Eds.), *The Pan-African Belt of NE Africa and Adjacent Areas*. Earth Evolution Science, Vieweg, Germany.

Fowler, A. R. and El-Kalioubi, B., (2004). Gravitational collapse origin of shear zones, foliations and linear structures in the Neoproterozoic cover nappes, Eastern Desert, Egypt. *Journal of African Earth Sciences* 38, 23–40.

Fritz, H., Wallbrecher, E., Khudier, A. A., Abu El Ela, F. and Dallmeyer, R.D., (1996). Formation of Neoproterozoic metamorphic core complexes during oblique convergence, Eastern Desert, Egypt. *Journal of African Earth Sciences* 23, 311–329.

Fritz, H., Dallmeyer, D.R., Wallbrecher, E., Loizenbauer, J., Hoinkes, G., Neumayr, P. and Khudeir, A. A., (2002). Neoproterozoic tectonothermal evolution of the central Eastern Desert, Egypt; a slow velocity tectonic process of core complex exhumation. *Journal African Earth Sciences* 34 (3/4), 137–155.

Fritz, H., Abdelsalam, M., Ali, K. A., Bingen, B., Collins, A. S., Fowler, A. R., Ghebreab, W., Hauenberger, C. A., Johnson, P. R., Kusky, T. M., Macey, P., Muhongo, S., Stern, R. G. and Viola, G., (2013). Orogen styles in the East African Orogen: a review of the Neoproterozoic to Cambrian tectonic evolution. *J. Afr. Earth Sci.* 86, pp. 65–106.

Garfunkel, Z., (1988). Relation between continental rifting and uplifting: evidence from the Suez rift and the northern Red Sea. *Tectonophysics* 150, 33–49.

Gass, I. G., (1982). Upper Proterozoic (Pan-African) Calc alkaline magmatism in northeastern Africa and Arabia. In: Thorp, R.S. (Ed.), *Andesites*. Wiley, New York, pp. 91–609.

Hassan, M. A. and Hashad, A. H., (1990). Precambrian of Egypt. In: Said, R. (Ed.), *The Geology of Egypt*. Balkema, Rotterdam, pp. 201–248.

Hassan, S., El Kazzaz, Y., Taha, M. and Mohammad, A., (2017). Late Neoproterozoic basement rocks of Meatiq area, Central Eastern Desert, Egypt: Petrography and remote sensing

characterizations. *Journal of African Earth Sciences* 14e31.

Ibrahim, S. and Cosgrove, J., (2001). Structural and tectonic evolution of the Umm Gheig/ El-Shush region, central Eastern Desert of Egypt. *Journal of African Earth Sciences*. 33, 199–209.

Kamel, M., Youssef, M., Hassan, M. and Bagash, F., (2016). Utilization of ETM+ Landsat data in geologic mapping of wadi Ghadir-Gabal Zabara area, Central Eastern Desert, Egypt. *The Egyptian Journal of Remote Sensing and Space Sciences* 19, pp. 343-360.

KrÖner, A., (1984). Late Precambrian tectonics and orogeny: A need to redefine the term Pan-African. In: KLERKX, J. ~z. MICHOT, J. (eds) *African Geology*. Musee Royal de l'Afrique Central Tervuren, Belgium, 23-28.

KrÖner, A., Krüger, J., and Rashwan, A. A., (1994). Age and tectonic setting of granitoid gneisses in the Eastern Desert of Egypt and southwest Sinai. *Geologische Rundschau*. 83, 502–513.

Lillesand, T. M. and Kiefer, R. W., (1979). Remote sensing and image interpretation. John Wiley and Sons, New York.

Lillesand, T. M. and Kiefer, R. W., (2000). Remote sensing and image interpretation (4th edn). John Wiley and Sons, New York.

Loughlin, W. P., (1991). Principal components analysis for alteration mapping. *Photogramm. Eng. Remote Sens.* 57, 1163e1169.

Neumayr, P., Hoinkes, G., Puhl, J., Mogessie, A. and Khudeir, A. A., (1998). The Meatiq dome (Eastern Desert, Egypt) a Precambrian metamorphic core complex petrological and geological evidence. *Journal of Metamorphic Geology* 16, 259–279.

Omar, G. I., Steckler, M. S., Buck, W. R. and Kohn, B. P., (1989). Fission track analysis of basement apatites at the western margin of the Gulf of Suez rift, Egypt; evidence for synchronicity of uplift and subsidence. *Earth Planetary Sci. Lett.* 94, 316–328.

Shalaby, A., (2010). The northern dome of Wadi Hafafit culmination, Eastern Desert, Egypt: structural setting in tectonic framework of a scissor-like wrench corridor. *Journal of African Earth Sciences* 57, 227–241.

Sonka, M., Hlavac, V. and Boyle, R., (1993). Image processing, Analysis and Machine vision. Chapman and Hall, London, 555 pp.

Stern R. J., (1993). Tectonic evolution of the late proterozoic East African Orogen: constraints from crustal evolution in the Arabian–Nubian Shield and the Mozambique Belt. In: Thorweihe U, Schandelmeier .H (eds) *Geoscientific Research in Northeast Africa*. Balkema, Rotterdam, pp 73–74.

Stern, R. J., (1994). Arc assembly and continental collision in the Neoproterozoic East-African Orogen — implications for the consolidation of Gondwanaland. *Annual Reviews of Earth and Planetary Sciences* 22, 319–351.

Stern, R. J. and Hedge, C. E., (1985). Geochronologic and isotopic constraints on Late Precambrian crustal evolution in the Eastern Desert of Egypt. *American Journal of Science* 285, 97–127.